Thermodynamic Analysis of Cascade Microcryocoolers with Low Pressure Ratios*

Ray Radebaugh

National Institute of Standards and Technology
Boulder, Colorado, 80305, USA

Abstract. The vapor-compression cycle for refrigeration near ambient temperature achieves high efficiency because the isenthalpic expansion of the condensed liquid is a rather efficient process. However, temperatures are limited to about 200 K with a single-stage system. Temperatures down to 77 K are possible with many stages. In the case of microcryocoolers using microcompressors, pressure ratios are usually limited to about 6 or less. As a result, even more stages are required to reach 77 K. If the microcompressors can be fabricated with low-cost wafer-level techniques, then the use of many stages with separate compressors may become a viable option for achieving temperatures of 77 K with high efficiency. We analyze the ideal thermodynamic efficiency of a cascade Joule-Thomson system for various temperatures down to 77 K and with low pressure ratios. About nine stages are required for 77 K, but fewer stages are also analyzed for operation at higher temperatures. For 77 K, an ideal second-law efficiency of 83 % of Carnot is possible with perfect recuperative heat exchangers and 65 % of Carnot is possible with no recuperative heat exchangers. The results are compared with calculated efficiencies in mixed-refrigerant cryocoolers over the range of 77 K to 200 K. Refrigeration at intermediate temperatures is also available. The use of single-component fluids in each of the stages is expected to eliminate the problem of pulsating flow and temperature oscillations experienced in microcryocoolers using mixed refrigerants.

Keywords: Cascade, cryocoolers, cryogenics, efficiency, heat exchangers, Joule-Thomson, microcompressors, recuperative, stages, vapor-compression cycle.

INTRODUCTION

Temperatures in the range of 77 K to 150 K are required for many microelectronic devices, such as infrared sensors, other photon detectors, high-temperature superconducting electronics, low-noise preamplifiers, and low-noise microgyroscopes. Refrigeration powers are typically about 10 mW to 100 mW. These devices are becoming much smaller than the existing cryocoolers available to cool them. To enable the use of these microelectronic devices in human-portable and micro-satellite applications, it becomes important to shrink the size of the cryocooler and reduce its mass. It is also important to maintain a high efficiency so that the battery size required for supplying power to the cryocooler can be kept very compact and last for a long time period. Generally the compressor is the largest item in a cryocooler, and it is especially true in the current development of microcryocoolers. Thus, to reduce the size of cryocoolers, we must pay close attention to what is required to reduce the compressor size. We first look at previous microcryocooler efforts to understand the state of the art and to learn where additional effort is required to reduce their size further, improve their efficiency, and modify them in a way to reduce cost through common mass-production techniques, such as wafer-level fabrication.

Development of microcryocoolers began in 1983 when Little first introduced a Joule-Thomson (JT) miniature (0.5×2×15 mm) cold finger made from glass slides with meandering flow channels about 10-20 μm deep abrasively-etched into the glass [1]. The working fluid was nitrogen gas supplied from a high-pressure (14 MPa) cylinder and vented to atmosphere at the exhaust. The cooler achieved a minimum temperature of 88 K and a net refrigeration power of 25 mW at 100 K by use of a flow rate of about 0.15 Std L/min (112 μmol/s). Similar microminiature refrigerators have been developed into commercial products.

The second effort in the development of microcryocoolers took place in 1998 at the University of Twente in the Netherlands. Holland, *et al.* [2] used a pair of glass capillaries for a miniature coaxial heat exchanger. The tubes had inner/outer diameters of 0.1/0.36 mm and 0.53/0.67 mm. Two heat exchangers were made, with lengths of 270 mm and 105 mm. The JT impedance was made with a wire inserted in the end of the inner high-pressure tube. With nitrogen supplied from a cylinder at an inlet pressure of 10 MPa, a low temperature of 82 K was achieved with both

coolers using a flow rate of 150 µmol/s for the longer one and 71 µmol/s for the shorter one. In 2000, Burger, *et al*. [3], also at the University of Twente, used the same capillary sizes, but shortened the cold head length to 77 mm. Ethylene was used as the refrigerant with an adsorption compressor for a closed system. The high-side pressure was 2.0 MPa, and the flow rate was 17.8 µmol/s. A refrigeration power of 200 mW was achieved at 170 K using a thermoelectric precooler at 238 K. In 2006 the Twente group switched to a planar glass geometry for the heat exchanger, expansion impedance, and evaporator by use of acid and abrasive etching to form two 50 µm flow channels between three parallel glass plates [4, 5]. The smallest cold head measured 2.2 mm wide by 28 mm long. A low temperature of 96 K was achieved with nitrogen from a cylinder expanding from a high pressure of 8 MPa to a low pressure of 0.6 MPa. The typical flow rate was about 36 µmol/s, which provided about 10 mW of cooling at about 100 K. The Twente group then developed a two-stage microcooler by use of the same microfabrication techniques [6]. The nitrogen first stage precooled a hydrogen stage to 94 K, and the hydrogen second stage reached 30 K. The high and low pressures for the nitrogen stage were 8.5 MPa and 0.1 MPa. The hydrogen stage used high and low pressures of 8.0 MPa and 0.1 MPa.

The previous work on microcryocoolers all relied on the use of rather high pressures (>8 MPa) and high pressure ratios (>80:1) provided by supply cylinders when no precooling was used. Even with the use of precooling to 238 K, a pressure ratio of 20:1 with an adsorption compressor was required to reach 170 K. Miniaturization of the complete cryocooler requires the use of a miniature compressor for a closed system. Ideally, such a compressor should be fabricated on a wafer using microfabrication techniques similar to those used in the cold head. Achieving that goal would lead to low-cost mass production of a complete microcryocooler. However, it is presently not possible to achieve such high pressure ratios in a microcompressor. A pressure ratio of about 4 is more realistic for a micromachined compressor. With that limitation in mind, a program at the University of Colorado and NIST/Boulder (CU/NIST) funded by DARPA focused on the use of mixed refrigerants in micro cryogenic coolers (MCCs). Optimized mixed refrigerants were found that could provide nearly an order of magnitude higher specific cooling powers (refrigeration per unit flow) compared with pure refrigerants for temperatures of 150 K for pressure ratios as small as 4 [7, 8]. A commercial, miniature rotary Stirling pressure oscillator was altered by blanking off the displacer drive and replacing the compressor top head with a head incorporating polyimide micro-check valves. Pressure ratios up to 7:1 were achieved with this miniature compressor, and flow rates of about 150 µmol/s (200 sccm) were produced when operated at a speed of 60 Hz. The isothermal efficiency peak of 17 % for the compressor occurred at a pressure ratio of 4 [9]. This compressor was then used to drive two different types of cold heads, both using five-component mixed refrigerants as the working fluid. The heat exchanger in the first version consisted of six hollow glass fibers inside a larger glass capillary as shown in Figure. 1. The cold head flow rate had a design value of 8 µmol/s to produce 15 mW of gross refrigeration and 10 mW of net refrigeration at about 150 K. Figure 2 shows the cold head attached to the compressor. It is clear from this picture that even this miniature compressor dominates the system size, and the compressor flow rate is much larger than necessary.

The glass fiber MCC discussed above is not readily manufacturable, but it provided valuable information on the use of mixed refrigerants in microcryocoolers. A new type of MCC was then developed by the CU/NIST team as

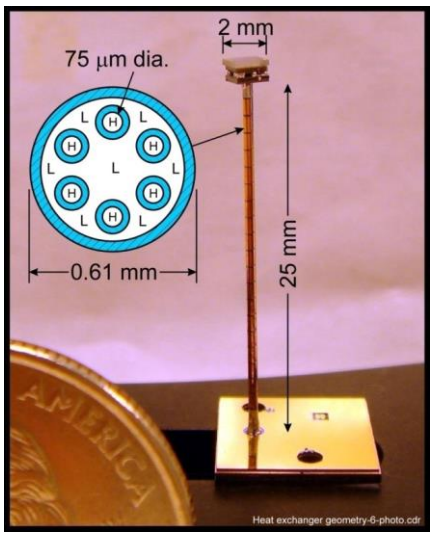

FIGURE 1. Glass heat exchanger and cold tip of Micro Cryogenic Cooler (MCC) for use with mixed refrigerants.

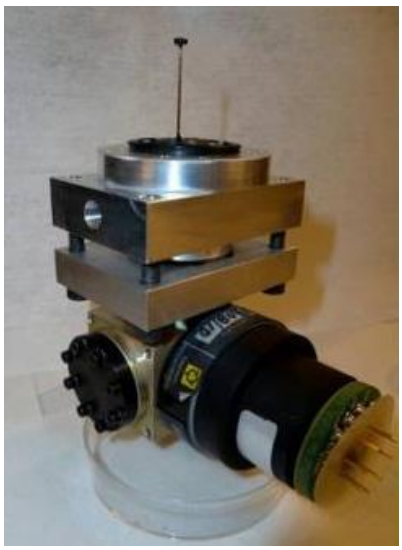

FIGURE 2. Glass MCC connected to modified miniature Stirling compressor [9].

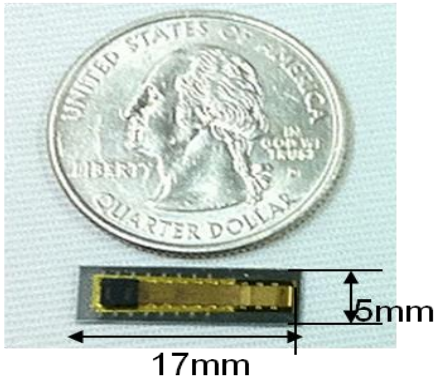

FIGURE 3. Planar polyimide cold head for use with mixed refrigerants at 200 K [10].

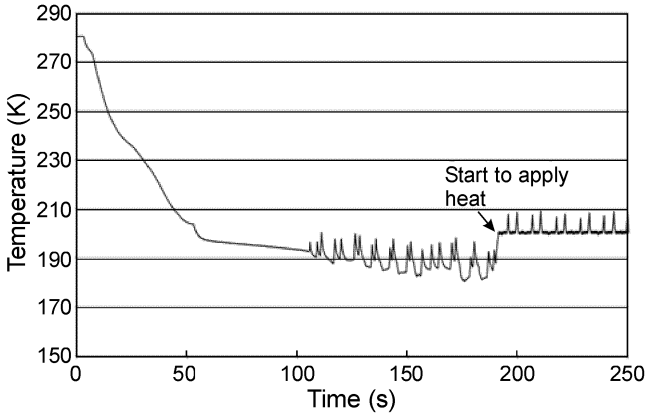

FIGURE 4. Cooldown behavior of polyimide cold head using mixed refrigerant optimized for 200 K showing temperature pulsations.

shown in Figure. 3. This planar cold stage is all polyimide, with the 10 μm flow channels formed using sacrificial copper [10,11]. It uses wafer-level fabrication techniques entirely. Polyimide also has the advantage of being flexible and having a thermal conductivity an order of magnitude lower than glass. The lower conductivity leads to a smaller coldhead, which in turn results in a reduced radiation heat load. This coldhead was also designed for a net refrigeration power of about 10 mW at 150 K driven by the modified Stirling compressor discussed above. Figure 4 shows an example cooldown curve with this coldhead using a five-component mixture optimized for 200 K, but the impedance was lower than the design value, so the flow rate was about four times larger than the design value. A low temperature of 190 K was achieved, but flow and temperature pulsations were experienced. The net refrigeration power at 200 K was 5.2 mW. The application of heat from a temperature controller could reduce the temperature fluctuations. Similar behavior was seen in the glass fiber MCC. Lewis *et al.* [12] has shown that the flow and temperature pulsations are a result of liquid slugs passing through the cold head that had built up in much larger void volumes between the compressor and the cold head. The liquid consisted mostly of the high boiling-point component. Ideally a two-phase flow should occur throughout most of the cold head. The deviation from ideal flow results in a significant reduction of the refrigeration power [12].

The instability associated with fluid mixtures in microscale geometries then caused us to start looking at pure fluids in a cascade cycle. A cascade cycle requires multiple compressors, which would be a big disadvantage unless the compressors could be mass produced using wafer-level fabrication techniques. Recent developments [13, 14] in micro vacuum pumps using wafer-level fabrication methods offer hope that similar techniques may result in microcompressors with a pressure ratio of at least 4. One of the DARPA-funded chip-scale vacuum micro pumps (CSVMP), as shown in Figure. 5, was able to provide a pressure ratio of 4.6 per stage in a two-stage roughing pump starting from atmospheric pressure [13]. Figure 6 shows a 24-stage roughing pump developed at the University of Michigan as part of the DARPA program on micro vacuum pumps [14]. However, valve problems prevented it from reaching its design vacuum level. The higher pressures in a compressor impose an even greater challenge in the development of the check valves for a microcompressor. The very limited flow rates possible with a chip-scale compressor require refrigerants with very high specific refrigeration powers. The next section compares specific refrigeration powers of various refrigerants.

FIGURE 5. Two-stage chip-scale vacuum micropump developed by MIT. Courtesy of DARPA.

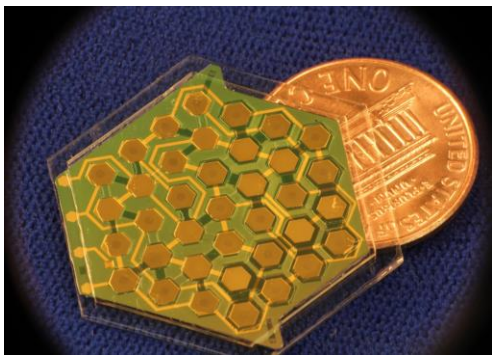

FIGURE 6. 24-stage chip-scale vacuum micropump developed by Univ. of Mich. Courtesy of DARPA.

COMPARISON OF SPECIFIC REFRIGERATION POWERS

The gross refrigeration power of any cycle not extracting work from the expanding fluid is given by [15]

$$\dot{Q}_r = \dot{n}(\Delta h_T)_{\min}, \tag{1}$$

where $\dot{n}$ is the molar flow rate and $(\Delta h_T)_{\min}$ is the minimum isothermal enthalpy difference between the high- and low-pressure streams over the temperature span between the low and high temperature. In Eq. (1) the parameter $(\Delta h_T)_{\min}$ is the specific refrigeration power. When losses, such as conduction, radiation, and heat exchanger ineffectiveness are subtracted from the gross refrigeration power, the result is the net refrigeration power $\dot{Q}_{net}$. Most of those losses are associated with the heat exchanger. To achieve a low flow and low compressor input power, the specific refrigeration power $(\Delta h_T)_{\min}$ should be as high as possible for a given refrigeration power. Figure 7 shows the isothermal enthalpy difference Δh_T for a pure refrigerant and two mixed refrigerants with a high pressure of 0.4 MPa and a low pressure of 0.1 MPa. For refrigeration at 150 K with a warm end at 300 K, R14 has a specific refrigeration power $(\Delta h_T)_{\min}$ of 0.10 kJ/mol, as shown in Fig. 7. The minimum value of Δh_T occurs at the warm end, which is typical of pure refrigerants. Fig. 7 also shows the isothermal enthalpy difference for two mixed refrigerants, one optimized for the temperature span of 140 K to 300 K and the other optimized for the span between 200 K and 300 K. We see that as the temperature span is decreased, $(\Delta h_T)_{\min}$ increases for the mixed refrigerants. For the temperature span of 150 K to 300 K, the mixed refrigerant has a much higher $(\Delta h_T)_{\min}$ than that of the pure, single-component refrigerant R14. A much higher pressure of 4 MPa is required to bring $(\Delta h_T)_{\min}$ for R14 up to that available with a mixed refrigerant. The critical temperature and pressure of R14 are 228 K and 3.75 MPa. The R14 curve in Fig. 7 shows that as the warm-end temperature drops below the critical temperature, $(\Delta h_T)_{\min}$ increases dramatically as the fluid liquefies at the high pressure, thus greatly reducing the high-pressure enthalpy. For a high pressure of 0.4 MPa, the warm-end temperature must be reduced to 169 K or lower to cause the high pressure R14 to condense into the liquid state. With such precooling, $(\Delta h_T)_{\min}$ increases to about 11 kJ/mol, which is much higher than that of the mixed refrigerant. As the precooling temperature is increased, the pressure required to achieve the high $(\Delta h_T)_{\min}$ associated with liquefaction increases considerably and becomes out of reach for a microcompressor.

THE VAPOR-COMPRESSION CYCLE

The refrigeration cycle in which the high pressure stream is condensed at ambient temperature is known as the vapor-compression cycle. This is the cycle that is used in household refrigerators and in most commercial refrigeration systems. Cold temperatures of about 250 K are typical, but pressure ratios of about 10 are usually

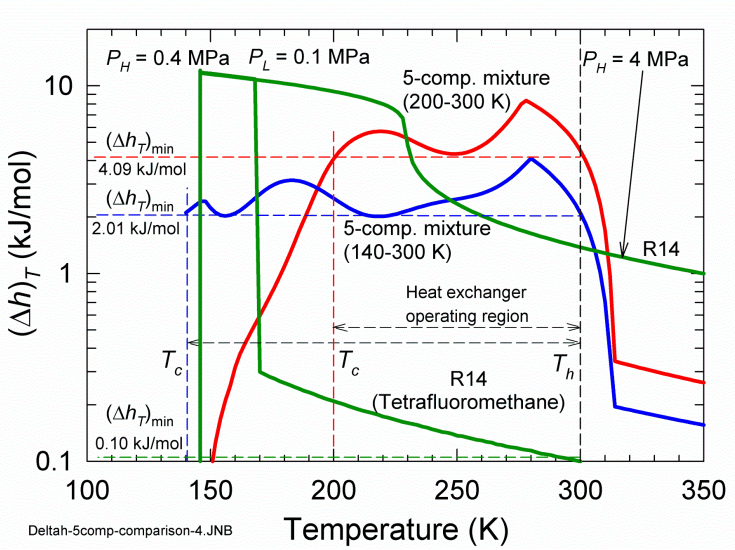

FIGURE 7. Isothermal enthalpy difference between high and low pressures for R14 and two mixed refrigerants. The specific refrigeration power equals the minimum Δh_T. The high Δh_T for R14 occurs when the high-pressure fluid liquefies.

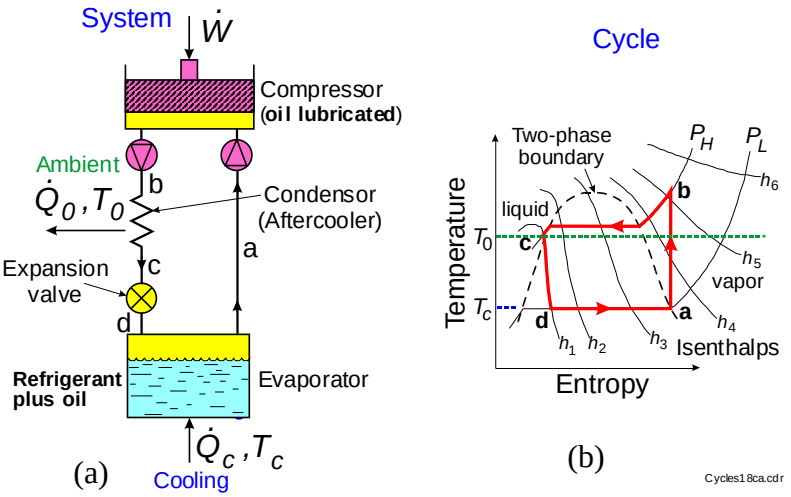

FIGURE 8. (a) Schematic of the vapor-compression cycle. (b) Vapor-compression cycle as shown on a temperature-entropy diagram. In this cycle the high pressure fluid condenses at ambient temperature.

required with the warm end at ambient. The cascade cycle consists of a series of vapor-compression cycles staged together to reach lower temperatures. Figure 8a is a schematic of the vapor-compression cycle, and Fig 8b shows the path followed by the refrigerant in a temperature-entropy diagram. The feature that distinguishes this cycle from the Joule-Thomson cycle is that the compression process occurs below the critical temperature of the fluid and at a pressure high enough to cause liquefaction. Thus, a high enthalpy difference is achieved at the warm end and is maintained as the temperature is lowered until the temperature reaches the saturation point of the low-pressure stream, often at the normal boiling point. As shown by Fig. 8b, the low temperature is achieved by isenthalpic expansion directly from the high temperature. No heat exchanger is required for any precooling, although a simple heat exchanger is often used to increase the efficiency somewhat. Oil-lubricated compressors are normally used in the cycle, because at 250 K the oil dissolved in the refrigerant does not freeze. However, when it is used for much lower temperatures, the oil must be removed from the refrigerant, or an oil-free compressor must be used. Temperatures significantly lower than 250 K would either require a compressor with a much higher pressure ratio, or more often, the use of a second stage with a different refrigerant. Any number of stages can be used to achieve even lower temperatures. Such a cycle is known as the cascade cycle and is investigated here for microcryocoolers.

THE CASCADE CYCLE FOR LOW PRESSURE RATIOS

High efficiency in the cascade cycle is achieved when the regions of high enthalpy difference of each stage overlap. Figure 9 shows an example of refrigerants suitable for use in a seven-stage cascade cycle to reach temperatures down to 100 K with a pressure ratio of about 4 for all stages. Only the Kr and R116 stages require a slightly higher pressure ratio as shown in the figure. A temperature of 150 K, commonly used for a new generation of infrared detectors, requires five stages. The specific refrigeration power $(\Delta h_T)_{\min}$ of the fifth stage is 11 kJ/mol, which is about five times that of the optimized mixed refrigerant for 150 K. In addition, heat leaks to the last stage are greatly reduced because the upper stages intercept them at higher temperatures. The upper stages have even higher specific refrigeration powers, so the required flow is greatly reduced. Table 1 lists refrigerants, temperatures, and pressures for a 16-stage cascade cycle capable of achieving 16 K. However, no pure refrigerant exists for the temperature range between 40 K and 67 K in stage 11. A mixed refrigerant containing neon, nitrogen, oxygen, and argon has shown promise of spanning this temperature range [16].

A schematic of a five-stage cascade cycle for a temperature of 145 K is shown in Figure. 10. The isothermal heat exchangers are shown as boxes with a solid line, whereas the recuperative heat exchangers are shown with dashed lines. Because each stage is a vapor-compression cycle, the recuperative heat exchangers are not necessary for operation of the cascade cycle. Instead, flow channels with low axial thermal conductivity can be used in place of the heat exchanger with some sacrifice in system efficiency. Elimination of the recuperative heat exchangers greatly simplifies the fabrication of the cold head by use of a planar geometry. All flow channels can then be on the same plane with copper strips used to conduct heat between stages at the isothermal heat exchangers. The high- and low-pressure streams change temperatures in steps instead of continuously if recuperative heat exchangers are in place.

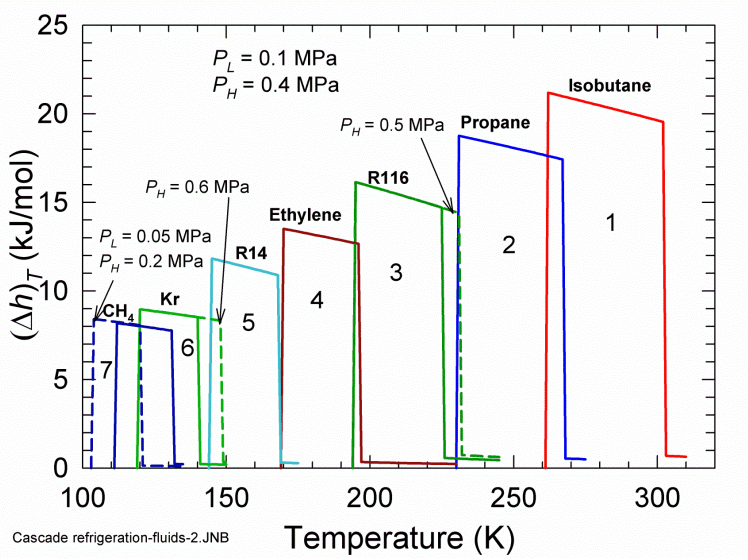

FIGURE 9. Overlapping large enthalpy differences for a set of fluids suitable for a 7-stage cascade cycle to 100 K.

Because the temperature change between stages is small when using the low pressure ratio of 4, the irreversible entropy generation in the isothermal heat exchangers is relatively small.

Thermodynamic Analysis of the Cascade Cycle

An element of the cascade cycle is shown in Figure. 11. Heat flows from this element of the isothermal heat exchanger due to ineffectiveness of the heat exchangers and due to real gas properties of the fluid. The heat is absorbed by the evaporator of the upper stage. In this analysis we assume the enthalpy change of the low-pressure stream between the hot and cold temperatures is less than that of the high-pressure stream. The heat exchanger pinch point is then at the warm end of all recuperative heat exchangers. This behavior always occurs for pure refrigerants for the low pressures considered here. That means for a perfect recuperative heat exchanger the high- and low-pressure streams have the same temperature at the warm end of the heat exchanger. Thus, the low-pressure flow from recuperative heat exchanger j+1 does not experience a temperature change or contribute a heat flow when entering the isothermal heat exchanger j. However, the enthalpy imbalance in recuperative heat exchanger j due to real gas effects means that the high-pressure stream experiences a temperature drop and contributes to heat flow

TABLE 1. Refrigerants, temperatures and pressures for a cascade cycle cooler with up to 16 stages using low pressure ratios.

Stage	**Refrigerant**	**Temperature** (K)	P_L (MPa)	P_H (MPa)
1	Isobutane (C_4H_{10})	261	0.1	0.4
2	Propane (C_3H_8)	231	0.1	0.4
3	R116 (C_2F_6) Hexafluoroethane	195	0.1	0.5
4	Ethylene (C_2H_4)	169	0.1	0.4
5	R14 (CF_4) Tetrafluoromethane	145	0.1	0.4
6	Krypton	120	0.1	0.6
7	Methane (CH_4)	104	0.05	0.2
8	Argon	87	0.1	0.4
9	Nitrogen	77	0.1	0.4
10	Nitrogen	67	0.025	0.1
11	Mixed refrigerant (Ne, N_2, O_2, Ar)	40	?	?
12	Neon	33	0.4	1.6
13	Neon	27	0.1	0.4
14	Neon	25	0.05	0.2
15	Hydrogen	20	0.1	0.4
16	Hydrogen	16	0.025	0.1

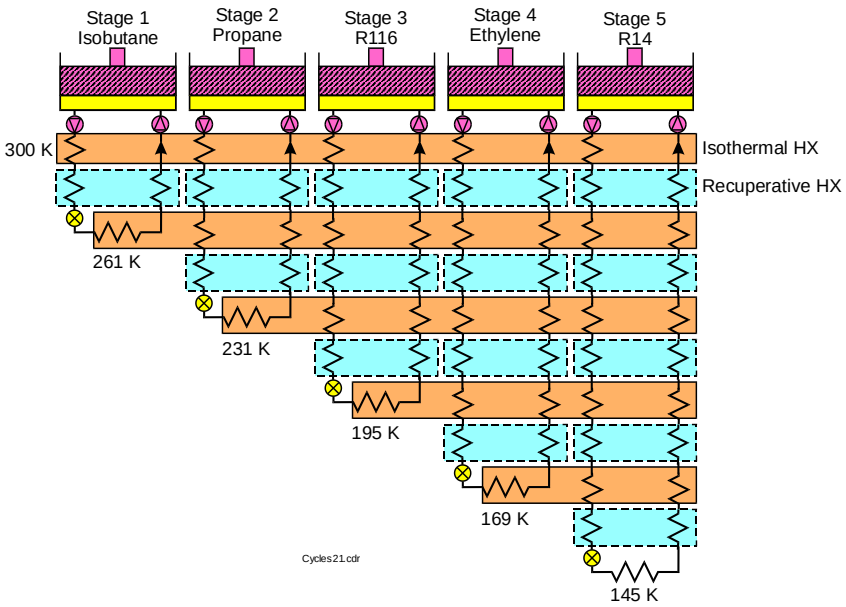

FIGURE 10. Schematic of a 5-stage cascade cycle cryocooler for a temperature of 145 K. Dashed lines around the recuperative heat exchangers indicate they can be eliminated with only a small decrease in system efficiency.

when entering the isothermal heat exchanger *j*. This heat flow that occurs with perfect heat exchangers is given by

$$\begin{aligned}(\dot{Q}_{i,j})_P &= \dot{n}[(h_h - h_c)_{H,i,j} - (h_h - h_c)_{L,i,j}] \\ &= \dot{n}[(h_L - h_H)_{c,i,j} - (h_L - h_H)_{h,i,j}] \\ &= \dot{n}[(\Delta h_c - \Delta h_h)_{i,j}],\end{aligned} \tag{2}$$

where *h* is the molar enthalpy. The subscripts *h* and *c* refer to the hot and cold ends. The subscripts *H* and *L* refer to the high- and low-pressure streams. For real recuperative heat exchangers with ineffectiveness λ, the heat flow from the isothermal heat exchanger *i,j* is given by

$$\dot{Q}_{i,j} = \dot{n}[(\Delta h_c - \Delta h_h)_{i,j} + \lambda_{i,j}(h_h - h_c)_{L,i,j} - \lambda_{i,j+1}(h_h - h_c)_{L,i,j+1}]. \tag{3}$$

The total precooling heat load on the evaporator of stage $i = k$ is

$$\dot{Q}_k = \sum_{i=k+1}^{n} \dot{Q}_{i,k}, \tag{4}$$

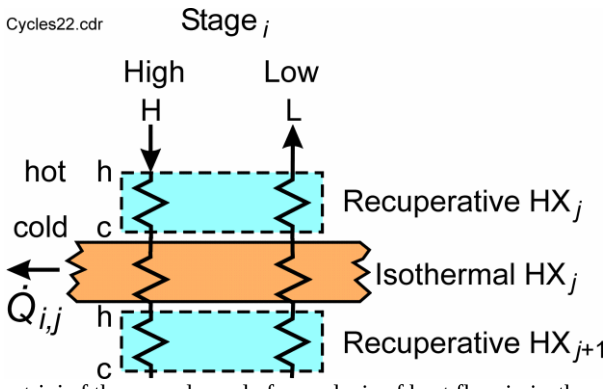

FIGURE 11. Element *i, j* of the cascade cycle for analysis of heat flow in isothermal heat exchangers.

where n is the number of stages. For example, the heat load on stage 3 is the sum of heat flows from isothermal heat exchanger 3 for stages 4 and 5. The gross refrigeration power at the cold end of stage k is given by Eq. (1), with $(\Delta h_T)_{\min}$ evaluated over the temperature range of the coldest recuperative heat exchanger of stage k. The ideal, reversible, isothermal power input to the compressor for stage k is given by

$$\dot{W}_{0,k} = \dot{n}_k \Delta g_{0,k}, \tag{5}$$

where Δg_0 is the change in the Gibbs free energy between the low and high pressures at ambient temperature. The total ideal compressor power is given by

$$\dot{W}_0 = \sum_{i=1}^{n} \dot{W}_{0,i}. \tag{6}$$

The system second law efficiency for ideal compressors is then

$$\varepsilon = \dot{W}_{0,Carnot} / \dot{W}_0, \tag{7}$$

where $\dot{W}_{0,Carnot}$ is the total ideal power input, assuming the Carnot power input for each stage.

RESULTS AND COMPARISONS

The calculated coefficient of performance *COP* and the second-law efficiency for various number of stages up to 9 (liquid nitrogen) are shown in Table 2 for perfect recuperative heat exchangers and for no recuperative heat exchangers. The compressors are assumed to be perfect with reversible, isothermal compression. The miniature compressor, modified from a miniature rotary Stirling cryocooler and discussed earlier for use with mixed refrigerants in a MCC, was measured to have an efficiency of 17 % at its peak performance. If chip-scale microcompressors can be developed with an efficiency of 20 %, then refrigeration at 77 K could be achieved with an efficiency of 13 % of Carnot with no recuperative heat exchangers and 16 % of Carnot with a 90 % effective recuperative heat exchanger.

Table 3 compares the calculated cascade-cycle performance for 145 K with that of a single-stage R14 JT cooler and a mixed-refrigerant JT cooler for the same temperature. The mixed refrigerant was optimized for 140 K. The *COP* and the second-law efficiency values are for the case where the recuperative heat exchanger has an ineffectiveness of 0, except for the last cascade case, in which no recuperative heat exchanger is used. The last column shows the maximum heat-exchanger ineffectiveness possible without losing all the gross refrigeration power. This maximum ineffectiveness is given by fluid properties as

$$\lambda_{\max} = (\Delta h_T)_{\min} / (h_h - h_c)_{\min}, \tag{8}$$

where the denominator is the minimum enthalpy difference between the hot and cold ends. The cascade cycle shown in the next-to-last row shows that the recuperative heat exchanger ineffectiveness can be greater than one for

TABLE 2. Thermodynamic performance of a cascade cycle cryocooler with low pressure ratio. Performance is shown for both a perfect recuperative heat exchanger and with no recuperative heat exchanger.

Stage	Cold Temperature (K)	Refrigerant	$(\Delta h_T)_{\min}$ (kJ/mol)	*COP* Perfect HX	ε Perfect HX	*COP* No HX	ε No HX
1	261	Isobutane	19.54	6.33	0.946	5.15	0.769
2	231	Propane	17.42	2.87	0.858	2.39	0.715
3	195	R116	14.38	1.64	0.884	1.32	0.708
4	169	Ethylene	12.66	1.15	0.889	0.936	0.726
5	145	R14	10.89	0.843	0.902	0.678	0.724
6	120	Krypton	7.83	0.551	0.831	0.460	0.692
7	104	Methane	8.06	0.448	0.850	0.365	0.693
8	87	Argon	6.05	0.355	0.868	0.291	0.711
9	77	Nitrogen	5.20	0.285	0.826	0.225	0.652

TABLE 3. Comparison of cycles and refrigerants for low and high temperatures of 145 K and 300 K with low and high pressures of 0.1 MPa and 0.4 MPa except for the second R14 case, in which a high pressure of 4.0 MPa is used.

Temperature Range	**Refrigerant (Mole fractions)**	$(\Delta h_T)_{min}$ **(kJ/mol)**	COP_{ideal}	η_{ideal} **%Carnot**	**HX ineff.** λ_{max}
145 – 300 K	R14 (T_{NBP} = 145 K) (Tetrafluoromethane)	0.100	0.0291	3.07	0.013
145 – 300 K	R14 (P_H = 4.0 MPa)	1.382	0.156	16.7	0.175
140 – 300 K	Methane: 0.34 N.B.P. 111.7 K Ethylene: 0.18 169.4 K Ethane: 0.20 184.6 K Isobutane: 0.16 261.4 K Isohexane: 0.12 333.4 K	2.01	0.601	68.6	0.085
145 – 300 K	Cascade (5 stages)	10.9-19.5	0.843	90.2	>1
145 – 300 K	Cascade (5 stages)	10.9-19.5	0.678	72.4	No HX

all stages and still provide net refrigeration. The last row shows the performance of the cascade cycle with no recuperative heat exchangers. We note that even though the mixed-refrigerant case is relatively efficient, the heat exchanger must be quite good to achieve an ineffectiveness significantly less than 0.085. The low ineffectiveness implies a relatively large heat exchanger and complex fabrication techniques. The efficiency of the single-component JT cooler is very low even with a high pressure of 4.0 MPa. The last row shows the high efficiency of the five-stage cascade cycle even when no recuperative heat exchanger is used. With a 20 % efficient compressor, refrigeration at 145 K can be achieved with an overall efficiency of 14 % of Carnot even with no recuperative heat exchanger.

CONCLUSIONS

Significant progress has been made in the last decade or so on the development of cold heads for microcryocoolers. These coldheads are made with glass or polyimide, and most have planar geometries that facilitate the use of microfabrication technologies. Early versions used high-pressure cylinders of single-component refrigerants at pressures of 8 MPa or more to provide the incoming high pressure. More recently, closed-cycle systems have been developed that use either adsorption compressors at high pressures of about 2 MPa or modified miniature Stirling compressors for pressure ratios of about 4 and mixed refrigerants optimized for low pressure ratios. The size of all these systems is dominated by that of the high-pressure source or compressor. The development of truly micro-sized complete closed-cycle cryocoolers awaits the development of microcompressors cabable of pressure ratios of at least 4. Ideally such compressors should be fabricated with wafer-scale processes for reduced costs in mass production. The availability of such microcompressors enables the development of microcryocoolers utilizing the cascade cycle. Because the cascade cycle uses the vapor-compression process of pure refrigerants, very high specific refrigeration powers can be achieved for each stage, which reduces the required flow rate of each compressor. The very high specific refrigeration power and the small temperature span also means the cooler operates efficiently even with no recuperative heat exchanger. Cooler fabrication is then greatly simplified. We have shown that with pressure ratios around 4, a temperature of 145 K can be achieved with five stages, and a temperature of 77 K uses nine stages. With a perfect compressor, the calculated second-law efficiencies are 72 % of Carnot for 145 K and 65 % of Carnot for 77 K when no recuperative heat exchangers are used. The efficiencies increase to 90 % and 83 % when a perfect heat exchanger is used. Even with compressor efficiencies of only 20 %, the system efficiency is still high with no recuperative heat exchangers. Thus, the cascade cycle warrants further development for use as microcryocoolers.

ACKNOWLEDGMENTS

Funding for this work came from the Micro Cryogenic Cooler (MCC) program of the DARPA Microsystems Technology Office with Dr. Nibir Dhar as the program manager. Prof. Y. C. Lee and Dr. Ryan Lewis of the University of Colorado are acknowledged for valuable discussions regarding MCCs and the cascade cycle.

REFERENCES

1. S. Garvey, S. Logan, R. Rowe, and W.A. Little, *Appl. Phys. Letters* **42**, 1048-1050 (1983).
2. H.J. Holland, J.F. Burger, N. Boersma, H.J.M. ter Brake, and H. Rogalla, *Cryogenics* **38**, 407-410 (1998).
3. J. Burger, H. Holland, J. Seppenwoodle, E. Berenschot, H. ter Brake, J. Gardeniers, M. Elwenspoek, and H. Rogalla, "165 K Microcooler Operating with a Sorption Compressor and Micromachined Cold Stage," *Cryocoolers 11*, Kluwer, New York, 2001, pp. 551-560.
4. P.P.P.M. Lerou, H.J.M. ter Brake, H.V. Jansen, J.F. Burger, H.J. Holland, and H. Rogalla, "Micromachined Joule-Thomson Coolers," *Advances in Cryogenic Engineering* **53**, American Institute of Physics, Melville, NY, 2008, pp. 614-621.
5. P.P.P.M. Lerou, G.C.F. Venborst, C.F. Berends, T.T. Veenstra, M. Blorn, J.F. Burger, H.J.M. ter Brake, and H. Rogalla, *J. Micromechanics and Micromachining* **16**, 1919-1925 (2006).
6. H.S. Cao, H.J. Holland, C.H. Vermeer, S. Vanapalli, P.P.P.M. Lerou, M. Blom, and H.J.M. ter Brake, *J. Micromech. Microeng.* **23**, 025014 (2013).
7. M.-H. Lin, P.E. Bradley, M.L. Huber, R. Lewis, R. Radebaugh, and Y.C. Lee, *Cryogenics* **50**, 439-442 (2010).
8. R. Lewis, Y. Wang, P.E. Bradley, M.L. Huber, R. Radebaugh, and Y.C. Lee, *Cryogenics* **54**, 37-43 (2013).
9. R. Lewis, "Testing and Analysis of Micro Cryogenic Coolers with Mixed Refrigerants," Ph.D. Thesis, Mech. Eng. Dept., University of Colorado, Boulder (2012).
10. Y. Wang, "Polymer-Based Micro Cryogenic Coolers," Ph.D. Thesis, Mech. Eng. Dept., University of Colorado, Boulder (2012).
11. Y. Wang, R. Lewis, R. Radebaugh, M.-H. Lin, and Y.C. Lee, "A Monolithic Polyimide Micro Cryogenic Cooler: Design, Fabrication, and Test," *J. Microelectromechanical Systems*, IEEE, to be published.
12. R. Lewis, Y. Wang, H. Schneider, Y.C. Lee, and R. Radebaugh, "Study of Mixed Refrigerant Undergoing Pulsating Flow in Micro Coolers with Precooling," *Cryogenics*, accepted for publication (2013).
13. H. Zhou, "A Study of Micromachined Displacement Pumps for Vacuum Generation," Ph.D. Thesis, Dept. of Electrical Engineering and Computer Science, Massachusetts Institute of Technology (2011).
14. A. Besharatian, "A Scalable, Modular, Multisatge, Peristaltic, Electrostatic Gas Micropump," Ph.D. Thesis, Electrical Engineering Dept., University of Michigan, Ann Arbor (2013).
15. R. Radebaugh, "Recent Developments in Cryocoolers," *19th International Congress of Refrigeration*, International Institute of Refrigeration (1995) pp. 973-989.
16. E. Luo, M. Gong, Y. Zhou, and L. Zhang, Experimental Investigation of a Mixed Refrigerant J-T Cryocooler Operating from 30 to 60 K," *Advances in Cryogenic Engineering* **45,** Kluwer, New York, 2000, pp. 315-321.